Journal of Mathematical Biology manuscript No.
(will be inserted by the editor)

Games of Age-Dependent Prevention of Chronic Infections by Social Distancing

Timothy C. Reluga and Jing Li

April 17, 2012

Abstract Epidemiological games combine epidemic modelling with game theory to assess strategic choices in response to risks from infectious diseases. In most epidemiological games studied thus-far, the strategies of an individual are represented with a single choice parameter. There are many natural situations where strategies can not be represented by a single dimension, including situations where individuals can change their behavior as they age. To better understand how age-dependent variations in behavior can help individuals deal with infection risks, we study an epidemiological game in an SI model with two life-history stages where social distancing behaviors that reduce exposure rates are age-dependent. When considering a special case of the general model, we show that there is a unique Nash equilibrium when the infection pressure is a monotone function of aggregate exposure rates, but non-monotone effects can appear even in our special case. The non-monotone effects sometimes result in three Nash equilibria, two of which have local invasion potential simultaneously. Returning to a general case, we also describe a game with continuous age-structure using partial-differential equations, numerically identify some Nash equilibria, and conjecture about uniqueness.

Keywords epidemiological games; social distancing; age structure

Mathematics Subject Classification (2000) 91A13, 91A10, 92D30, 92D25

1 Introduction

One of the contemporary theoretical challenges in behavioral epidemiology is to determine the best individual practices for cooping with an infectious disease. Naively, we hope to determine simple and regular behavior patterns that are optimal for individuals, easily coordinated based on general disease properties, and lead to stable outcomes. Such theoretically-determined behaviors could then be unanimously endorsed as goals of public-health programs.

A number of authors have made theoretical studies of this problem, based on a variety of epidemiological assumptions. Recently, Reluga et al. (2007) studied a game of behavior choice for a simple disease model where the virulence of infection depends on age. The results showed that when the virulence in juveniles is larger than in adults, the Nash equilibria is to minimize exposure rates, but when the virulence in juveniles is less than the virulence in adults, both minimizing and maximizing exposure rates can be Nash equilibria. This is a clear challenge to our hopes of finding universal behavior patterns. However, a major limitation of that theory is that individuals are assumed to use the same behaviors as both juveniles and adults. No studies have yet addressed the robustness of those equilibria under age-dependent variations in behavior. In the most common epidemiological games concerned with disease transmission, only one player type is considered, and this player type has only a scalar strategy set (Reluga and Galvani, 2011). Some research considers games with two or

Timothy C. Reluga
Department of Mathematics, Department of Biology, Pennsylvania State University
University Park, PA 16802, USA
E-mail: timothy@reluga.org
Jing Li
Department of Mathematics, Pennsylvania State University
University Park, PA 16802, USA

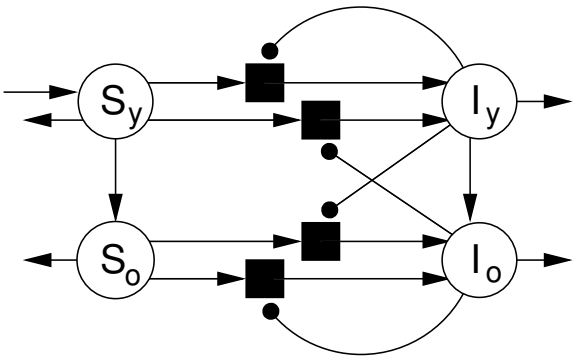

Fig. 1 This hypergraph represents the reaction network of System (1). Arrows indicate mass flow, while lines ending in discs identify catalytic interactions.

more player types (Brito et al., 1991; Chen, 2004; Reluga, 2009; Cornforth et al., 2011). Only a couple of studies (Chen, 2006; Reluga, 2010) have considered games where strategies are elements of vector spaces with two or more dimensions. There may be many scenarios where uniqueness can be restored through age-specific variation.

Here, we set out to explore this area of mathematical epidemiology further by investigating two games where the player strategies can change as their ages change. The methods we use are the same as those commonly used in theoretical evolutionary biology to study life history and behavior (Clark and Mangel, 2000; Charlesworth, 1994; Houston and McNamara, 1999; McNamara et al., 2001). They differ, though, in that strategies are not restricted by inheritance, and we have explicit nonlinear models of disease dynamics.

Our susceptible-infected (SI) disease-transmission models are variations of the age-structure approaches described by Schenzle (1984). In the first analysis, an SI model with two age classes is considered. We use this SI model as part of an epidemiological social-distance game where the reduction in exposure risk is a linear function of individual investment. The utility function is determined, game equilibria are identified in several special cases, and a numerical algorithm is supplied for the general case. We will find that under some natural hypotheses, as long as the infection pressure decreases monotonely in response to decreases in exposure rate, there is a unique Nash equilibrium. As in (Reluga et al., 2007), there can be multiple Nash equilibria. However, when behaviors can vary with age, age-dependent differences in cost alone can not generate multiple equilibria. The existence of multiple equilibria requires mechanisms where the reductions in exposure rates increase the infection pressure.

In the second game, we consider an SI model of disease-transmission with continuous age structure. The model is formulated with general age-structure for transmission and recovery. Although elements of the strategy set are functions of age, this is not a differential-game in the classic sense, as all the analysis is undertaken at the temporal steady-state of the system. Numerical results are presented in the special case of a Gompertzian mortality hypothesis.

The paper closes with a discussion of the limitations of these two models and directions for future research. The major result of these analyses is that age-dependent variations in behavior have competing effects. An age-specific increase in social-distancing reduces the risk of infection per contact, but also increases the susceptible pool of individuals at older ages. Depending on the patterns of susceptibility and transmissibility, this may lead to greater infection pressures. The competing effects of greater infection pressure but lower risk per contact define a potentially non-monotone response profile leading to two or more stable behavioral equilibria. Future research will be needed to further parse the practical importance of these phenomena.

2 Two-Stage Age-Structure

To study age-dependent behaviors in one of their simplest contexts, we propose an SI model of an infectious disease with properties inspired by HIV: chronic infection, low transmission rate, no cures or vaccines. Suppose this disease is transmitted in a population subdivided into two age-groups; young people who are susceptible (S_y) or infected (I_y), and old people who are susceptible (S_o) or infected (I_o). Without infection, young people become old at rate f and die from background causes at rate m_y; Old people die from background causes at rate $m_o > m_y$. Infected people remain infected for the rest of their lives and infection increases mortality rates. Young and old people who are infected die at rates γ_y and γ_o respectively. Individuals become infected at a

Table 1 The list of all symbols used in System (1).

Symbol	Interpretation
S_y	young susceptible people
I_y	young infected people
S_o	old susceptible people
I_o	old infected people
r	birth rate of the population
f	maturation rate of the population
m_y	background death rate of young people
m_o	background death rate of old people
γ_y	death rate of infected young people
γ_o	death rate of infected old people
$\overline{\sigma}_y$	the aggregated effective exposure rate in the young population
$\overline{\sigma}_o$	the aggregated effective exposure rate in the old population
λ_y	the infection pressure in the young population
λ_o	the infection pressure in the old population
β_{ij}, $i,j \in \{y,o\}$	the disease transmission rate from age group j to i

rate depending on the infection pressure and the effective exposure to risky events at each age. The infection pressure $\lambda = \langle \lambda_y, \lambda_o \rangle$ with $\lambda_j := \beta_{jy} I_y + \beta_{jo} I_o$ for each age group $j \in \{y, o\}$, while the aggregated effective exposure rates are $\overline{\sigma}_y$ in the young subpopulation and $\overline{\sigma}_o$ in the old subpopulation. The angle-bracket notation $\langle , \rangle$ will be used throughout this paper to represent vectors. We adopt this to avoid confusion with the bracket notation $[,]$ for intervals that we will also use.

At the population scale, the dynamics are governed by the system of differential equations

$$\dot{S}_y = r - \overline{\sigma}_y \lambda_y S_y - m_y S_y - f S_y, \tag{1a}$$

$$\dot{I}_y = \overline{\sigma}_y \lambda_y S_y - (\gamma_y + f) I_y, \tag{1b}$$

$$\dot{S}_o = f S_y - \overline{\sigma}_o \lambda_o S_o - m_o S_o, \tag{1c}$$

$$\dot{I}_o = f I_y + \overline{\sigma}_o \lambda_o S_o - \gamma_o I_o. \tag{1d}$$

The corresponding reaction network is depicted in Figure 1. A summary of the symbols used in System (1) is given in Table 1. This model is similar to that of (Reluga, 2009), but differs in the inclusion of aging and demographic turnover which pumps individuals into the youngest age group, and changes the game by unifying everybody into a single population.

Now, consider a single person from this population. The state of a single person changes according to a continuous-time Markov process. The probability that an individual occupies any state at time t is given by a vector $\mathbf{p}(t)$ with

$$\dot{\mathbf{p}} = \mathbf{Q}\mathbf{p} \tag{2}$$

where the transition-rate matrix for an individual is

$$\mathbf{Q} := \begin{bmatrix} -\sigma_y \lambda_y - m_y - f & 0 & 0 & 0 \\ \sigma_y \lambda_y & -\gamma_y - f & 0 & 0 \\ f & 0 & -\sigma_o \lambda_o - m_o & 0 \\ 0 & f & \sigma_o \lambda_o & -\gamma_o \end{bmatrix}. \tag{3}$$

Each individual is initially susceptible and young, so the initial state of the Markov process is given by $\mathbf{p}(0) = \langle 1, 0, 0, 0 \rangle$. Individuals can invest in behavior-changes that reduce their personal effective exposure rates $\sigma = \langle \sigma_y, \sigma_o \rangle$ when the individual is young or old respectively. An individual's exposure rates σ may differ from the aggregate exposure rates $\overline{\sigma} = \langle \overline{\sigma}_y, \overline{\sigma}_o \rangle$.

To calculate the payoff of a strategy choice, we associate costs and benefits with residence in each state and with changes in exposure. Individuals accumulate u_y and u_o units of benefit per year while they reside in young and old states respectively. While sick, they pay annual costs c_{iy} if young and c_{io} if old. While healthy, young and old individuals make annual investments π_y and π_o to protect themselves and reduce their effective exposure rates. Together, the annual utility gains of each state are represented by the vector

$$\mathbf{v} = \langle u_y - \pi_y, u_y - c_{iy}, u_o - \pi_o, u_o - c_{io} \rangle. \tag{4}$$

Applying standard theory (Reluga and Galvani, 2011), the utility is given by

$$\mathcal{U} := \mathbf{v}^{\mathrm{T}} \int_0^\infty e^{-ht}\mathbf{p}(t)dt = \mathbf{v}^{\mathrm{T}} \int_0^\infty e^{-ht}e^{\widetilde{\mathbf{Q}}t}\mathbf{p}(0)dt = \mathbf{v}^{\mathrm{T}} \left(h\mathbf{I} - \widetilde{\mathbf{Q}}\right)^{-1} \mathbf{p}(0), \tag{5}$$

where h is the discounting rate, and $\widetilde{\mathbf{Q}}$ is $\mathbf{Q}$ evaluated at a steady-state of System (1). Our age-structured SI game is closely related to SIR and SIS games, and can be extended to represent those cases.

The analysis conducted here makes use of two sets of hypotheses. The first set of hypotheses encodes our common expectations about the effects of chronic infection.

Hypothesis 1 *The epidemiology of the infectious disease system under study satisfies the following properties.*

1a. The population is large enough to maintain endemic disease transmission: $\mathcal{R}_0 > 1$ *(see Appendix A for the definition of* $\mathcal{R}_0$*.)*

1b. Disease mortality rates are faster than background mortality rates:

$$0 < m_y < \gamma_y \quad \textit{and} \quad 0 < m_o < \gamma_o.$$

1c. Infection is not beneficial: $0 \le c_{iy}$ *and* $0 \le c_{io}$*.*

The second set of hypotheses restricts the generality of our model while facilitating its mathematical analysis.

Hypothesis 2 *Assume that*

2a. The infection pressure is the same in both age groups:

$$\begin{aligned} \beta_y &:= \beta_{yy} = \beta_{oy}, \\ \beta_o &:= \beta_{yo} = \beta_{oo}, \\ \lambda = \lambda_y &= \lambda_o = \beta_y I_y + \beta_o I_o. \end{aligned}$$

2b. The effective exposure rates depend on personal investments in prevention according to

$$\begin{aligned} \sigma_y(\pi_y) &= \max\left\{0, 1 - \frac{\pi_y}{c_{py}}\right\}, \\ \sigma_o(\pi_o) &= \max\left\{0, 1 - \frac{\pi_o}{c_{po}}\right\}. \end{aligned}$$

2c. No discounting is used when accounting for future returns: $h = 0$*.*

The parameters c_{py} and c_{po} represent the minimum investment needed to stop personal exposure when young or old, respectively. Mathematically, it will be convenient to treat the effective exposure rates σ as the strategies chosen by individuals. Under Hypothesis 2, we may assume $\sigma = \langle \sigma_y, \sigma_o \rangle$ is an element of the strategy set $[0,1] \times [0,1]$ without further loss of generality. Then the amount invested to reduce exposure

$$\pi_j = (1 - \sigma_j)c_{pj},\ j \in \{y, o\}. \tag{6}$$

In the limiting cases of $c_{pj} \to 0$, the related exposure rate σ_j can be varied over its full domain $[0,1]$ without any cost.

Under Hypotheses 1 and 2, the utility function depends on the exposure rates according to

$$\mathcal{U}(\sigma, \widetilde{\lambda}(\overline{\sigma})) = \frac{u_y - (1-\sigma_y)\,c_{py} + \widetilde{\lambda}\sigma_y w_{iy} + f\left[\dfrac{u_o - (1-\sigma_o)\,c_{po} + \sigma_o\widetilde{\lambda}w_{io}}{m_o + \widetilde{\lambda}\sigma_o}\right]}{m_y + f + \widetilde{\lambda}\,\sigma_y} \tag{7a}$$

where $\widetilde{\lambda}$ is the stationary infection pressure solving the steady-state condition for the given $\overline{\sigma}$ (see Appendix A Eq. (44)),

$$w_{iy} := \frac{u_y - c_{iy} + f w_{io}}{\gamma_y + f}, \tag{7b}$$

$$w_{io} := \frac{u_o - c_{io}}{\gamma_o}. \tag{7c}$$

Note that w_{iy} and w_{io} represent the expected lifetime utility of being sick when young or old, respectively. Hypothesis 1 implies that, without investment in protection, being sick is always worse than being healthy in the sense that

$$\frac{u_y + f w_{io}}{m_y + f} \geq w_{iy}, \tag{8a}$$

$$\frac{u_o}{m_o} \geq w_{io}. \tag{8b}$$

The relative utility of σ compared to $\overline{\sigma}$ is defined as $\mathcal{U}(\sigma, \widetilde{\lambda}(\overline{\sigma}))/\mathcal{U}(\overline{\sigma}, \widetilde{\lambda}(\overline{\sigma}))$.

2.1 Best Responses

Given the utility $\mathcal{U}(\sigma, \widetilde{\lambda}(\overline{\sigma}))$, we can now ask the questions about what types of equilibria the population game possesses, how to calculate these equilibria, and how those equilibria depend on the transmission rate, the removal rate, the costs of infection, and the costs of exposure-reduction. We expect this to be more difficult than analyses with scalar strategies because we have to analyze the utility function on a four-dimensional domain that can not be represented visually.

As we show in Appendix A, the stationary infection pressure $\widetilde{\lambda}$ of System (1) is a uniquely defined function of the aggregated exposure rate $\overline{\sigma}$. For a given stationary infection pressure, the best-response correspondence

$$\sigma^B := \operatorname{argmax}_\sigma \mathcal{U}(\sigma, \widetilde{\lambda}(\overline{\sigma})). \tag{9}$$

A summary of some relevant properties of correspondences is provided in Appendix B. The best response correspondence can be found by differentiating the utility function with respect to individual strategies:

$$\sigma^B = H\left(\frac{u_y + \widetilde{\lambda} w_{iy} + f E_o}{m_y + f + \widetilde{\lambda}} - \frac{u_y - c_{py} + f E_o}{m_y + f}\right) \times H\left(\frac{u_o + \widetilde{\lambda} w_{io}}{m_o + \widetilde{\lambda}} - \frac{u_o - c_{po}}{m_o}\right) \tag{10a}$$

where

$$E_o := \max_{\sigma_o \in [0,1]} \frac{u_o - (1 - \sigma_o)(c_{po}) + \sigma_o w_{io} \widetilde{\lambda}}{\left(m_o + \widetilde{\lambda}\, \sigma_o\right)} \tag{10b}$$

and the Heaviside correspondence

$$H(x) := \begin{cases} \{0\} & \text{if } x < 0, \\ [0,1] & \text{if } x = 0, \\ \{1\} & \text{if } x > 0. \end{cases} \tag{10c}$$

So σ^B is a set of vectors represented as the Cartesian product of sets returned by the Heaviside correspondences. Because the utility function is a ratio of two expressions linear in σ, the set of best responses σ^B consists of only points on the boundary of the strategy set except in special cases where $\mathcal{U}$ is flat. The utility is flat only if the arguments of both Heaviside correspondences in Eq. (10) vanish simultaneously. This can occur in three different situations. First, if $c_{py} > 0$ and $c_{po} > 0$,

$$\frac{u_y - c_{py}}{m_y + f} - w_{iy} + \frac{(u_o - c_{po})\, f}{m_o\,(m_y + f)} = \left(\frac{u_o - c_{po}}{m_o} - w_{io}\right) \frac{c_{py}}{c_{po}} \tag{11a}$$

and

$$\widetilde{\lambda} = \frac{m_o c_{po}}{u_o - m_o w_{io} - c_{po}}, \tag{11b}$$

then

$$\mathcal{U} = \frac{(u_y - c_{py}) + f \frac{(u_o - c_{po})}{m_o}}{m_y + f}. \tag{12}$$

This may occur for feasible parameter values. Second, if $c_{py} = c_{po} = 0$ and $\widetilde{\lambda} = 0$, then $\mathcal{U}$ is flat because there is no cost to prevention and no risk of infection. Third, if $c_{py} = c_{po} = (u_o - w_{io}m_o)/(1-\sigma_o)$ and $\widetilde{\lambda} = -m_o/\sigma_o$, then $\mathcal{U}$ is flat, but this situation is not biologically meaningful under Hypotheses 1 and 2.

There are a few mathematical results regarding best-responses that will be useful as we proceed. First, $\sigma^B(\widetilde{\lambda})$ is upper semi-continuous, although it is not lower semi-continuous (see Appendix B). The best response is also monotone-decreasing in the infection pressure provided being sick is worse than being healthy.

Lemma 1 *$\sigma^B(\widetilde{\lambda})$ is monotone decreasing in $\widetilde{\lambda}$.*

Proof Our lemma can be proven from inspection of Eq. (10). Under Hypotheses 1 and 2, the inequalities in Eq. (8) hold. Consider

$$\frac{u_o + \widetilde{\lambda} w_{io}}{m_o + \widetilde{\lambda}} - \frac{u_o - c_{po}}{m_o} = \frac{(\frac{u_o}{m_o})m_o + \widetilde{\lambda} w_{io}}{m_o + \widetilde{\lambda}} - \frac{u_o - c_{po}}{m_o}. \tag{13}$$

By Eq. (8b), we know this is decreasing in $\widetilde{\lambda}$. The Heaviside correspondence is increasing (see Appendix B), so $\sigma_o^B(\widetilde{\lambda})$ must be decreasing.

Next, for any nonnegative a and b with $a + b > 0$ and $g_b \geq g_a \geq 0$, $g_a \leq (ag_a + bg_b)/(a+b) \leq g_b$, so

$$\left.\frac{u_o - (1-\sigma_o)\, c_{po} + \sigma_o w_{io}\widetilde{\lambda}}{\left(m_o + \widetilde{\lambda}\,\sigma_o\right)}\right|_{\sigma_o = 1} = \frac{(\frac{u_o}{m_o})m_o + w_{io}\widetilde{\lambda}}{\left(m_o + \widetilde{\lambda}\right)} \geq w_{io} \tag{14}$$

by Eq. (8b). This implies $E_o \geq w_{io}$. Now,

$$\frac{u_y + \widetilde{\lambda} w_{iy} + fE_o}{m_y + f + \widetilde{\lambda}} - \frac{u_y - c_{py} + fE_o}{m_y + f} = \frac{\widetilde{\lambda} w_{iy} - \widetilde{\lambda}\left(\dfrac{u_y + fE_o}{m_y + f}\right)}{m_y + f + \widetilde{\lambda}} + \frac{c_{py}}{m_y + f}. \tag{15}$$

Since $E_o \geq w_{io}$, Eq. (8a) implies that this is decreasing in $\widetilde{\lambda}$. It follows that $\sigma_y^B(\widetilde{\lambda})$ is also decreasing in $\widetilde{\lambda}$. QED

Further, we can identify the extreme best responses. If the stationary infection pressure $\widetilde{\lambda} = 0$, then

$$\sigma^B = H\left(\frac{c_{py}}{m_y + f}\right) \times H\left(\frac{c_{po}}{m_o}\right). \tag{16}$$

As long as self-protection is not free (c_{py} and c_{po} are positive), $\widetilde{\lambda} = 0$ implies $\sigma^B = \{1\} \times \{1\}$. The asymptotic limit for large infection pressure depends on the relative costs of infection w_{iy} and w_{io}. If old people are better off infected than protecting themselves ($w_{io} > (u_o - c_{po})/m_o$), then

$$\lim_{\widetilde{\lambda}\to\infty} \sigma^B(\widetilde{\lambda}) = H\left(w_{iy} - \frac{u_y - c_{py} + fw_{io}}{m_y + f}\right) \times \{1\} \tag{17}$$

If old people are worse off infected ($w_{io} < (u_o - c_{po})/m_o$), then

$$\lim_{\widetilde{\lambda}\to\infty} \sigma^B(\widetilde{\lambda}) = H\left(w_{iy} - \frac{u_y - c_{py}}{m_y + f} - \frac{f}{m_y + f}\left[\frac{u_o - c_{po}}{m_o}\right]\right) \times \{0\}. \tag{18}$$

2.2 Game equilibria

We can now proceed with identifying solutions to the population game described by Eq. (7a). Nash equilibria are strategies which are best responses to themselves. A strategy σ^* is a Nash equilibrium if it is a solution of the set inclusion relation

$$\sigma^* \in \sigma^B(\widetilde{\lambda}(\sigma^*)). \tag{19}$$

The first important result is that if being sick is worse than being healthy and shortens your life, no matter when you get sick, then everybody will adopt all the exposure-reducing measures available if there is no cost to reducing exposure.

Theorem 1 *$\sigma^* = \langle 0, 0\rangle$ is a Nash equilibrium of Eq.* (7a) *if and only if $c_{py} = c_{po} = 0$.*

Proof From Hypothesis 1, Lemma 1 implies that σ^B is monotone decreasing in $\widetilde{\lambda}$. If $c_{py} = c_{po} = 0$, then from Eq. (16) and monotonicity, we know that $\langle 0, 0\rangle \in \sigma^B(\widetilde{\lambda})$ for every $\widetilde{\lambda} \geq 0$. If $\overline{\sigma} = \langle 0, 0\rangle$, then the stationary solution analysis (Eq. (42) and Eq. (44) of Appendix A), $\widetilde{\lambda} = 0$. Thus, $\sigma^* = \langle 0, 0\rangle$ solves Eq. (19), and is a Nash equilibrium.

If $c_{py} > 0$ or $c_{po} > 0$, then from Eq. (16), $\langle 0, 0\rangle$ is not a best-response to itself, and thus not a Nash equilibrium.

QED

Every other strategy for which $\widetilde{\lambda} = 0$ is also a Nash equilibrium when $c_{py} = c_{po} = 0$, so $\langle 0, 0\rangle$ is not unique. It is a corner of a simply connected set of Nash equilibria.

Our second important result is that Eq. (19) can be analyzed directly to show that reducing one's exposure is counter-productive if the cost of reducing exposure is too large.

Theorem 2 *If $c_{py} > 0$, $c_{po} > 0$, and*

$$w_{io} > \frac{u_o - c_{po}}{m_o}, \tag{20a}$$

$$w_{iy} > \frac{u_y - c_{py} + fE_o}{m_y + f}, \tag{20b}$$

then $\sigma^* = \langle 1, 1\rangle$ is the unique Nash equilibrium of Eq. (7a).

The inequalities (20a) and (20b) can be interpreted in the sense that being sick when you are old is better than protecting yourself, and getting sick when you are young is better than protecting yourself and doing your best to protect yourself when you are old, respectively. Under these two conditions, it is always best to do nothing.

Proof By substituting these conditions into Eq. (10) and we see that (20b) and (20a) ensure the positivity of the arguments of the Heaviside functions in Eq. (10), respectively, which implies that $\sigma^B = \langle 1, 1\rangle$ is the unique best response for all $\widetilde{\lambda} \geq 0$. Thus, it is the only strategy that is a best response to itself. Thus, it is the unique solution to Eq. (19).

QED

The result is not tight, as there are costs below the thresholds of Theorem 2 for which $\langle 1, 1\rangle$ is still the unique Nash equilibrium. The tight condition depends on the maximum infection pressure when $\overline{\sigma} = \langle 1, 1\rangle$, which requires solving for the stationary solutions explicitly.

Theorems 1 and 2 are only useful for extreme values of the costs c_{py} and c_{po}. For intermediate values of these costs, the analysis can be more complicated. This is in-part due to the vector form of Eq. (19). By mapping best responses to their matching stationary infection pressures, we can reduce the vector relation to a scalar relation for the infection pressure at Nash equilibrium:

$$\widetilde{\lambda}(\sigma^*) \in \lambda(\sigma^B(\widetilde{\lambda}(\sigma^*))). \tag{21}$$

Our first application of Eq. (21) is to prove there is always a Nash equilibrium.

Theorem 3 *If $c_{py} > 0$ and $c_{po} > 0$, then there exists a Nash equilibrium.*

Proof Under the stated assumptions plus Hypothesis 1, $\lambda(\sigma^B(0)) > 0$ and from Eq. (45) in Appendix A, $\lim_{l\to\infty} \lambda(\sigma^B(l))$ is finite. By the upper semi-continuity of σ^B, and the continuity of $\lambda(\sigma)$, the intermediate value theorem ensures at least one solution to Eq. (21). If we use both sides as arguments to σ^B, we must also then have

$$\sigma^B(\widetilde{\lambda}) \subseteq \sigma^B(\lambda(\sigma^B(\widetilde{\lambda}))). \tag{22}$$

Thus, existence of a solution to Eq. (21) also implies existence of a solution to Eq. (19).

QED

Algorithm 1 Calculate the set Σ^* of Nash equilibria of Eq. (7a) when $c_{py}c_{po} > 0$

$\Sigma^* \leftarrow \{\}$
if $\mathcal{R}_0 \leq 1$ **then**
  $\Sigma^* \leftarrow \Sigma^* \cup \{\langle 1, 1\rangle\}$
else
  Calculate the set of solutions Λ to Eq. (21) using a scalar root-finding subroutine. {*We expect this to be as finite set of isolated points.*}
  for all $x \in \Lambda$ **do**
    Calculate the set of best responses $\sigma^B(x)$
    Use scalar root-finding to find $S \leftarrow \{y \in \sigma^B(x) : x = \widetilde{\lambda}(y)\}$.
    $\Sigma^* \leftarrow \Sigma^* \cup S$
  end for
end if
return Σ^*

This can be strengthened to non-negative prevention-costs without much trouble. Having established existence, let's now consider the question of uniqueness. The infection-pressure inclusion given as Eq. (21) can be solved using standard 1-D root-finding methods. We can then invert $\widetilde{\lambda} = \lambda(\sigma^*)$ to find σ^* and verify that the strategies satisfy Eq. (19). So, using Eqs. (19) and (21), we can construct an algorithm for determination of all local Nash equilibria (see Table 1).

Thus, the problem of identifying Nash equilibria of Eq. (7a) is equivalent to a scalar root-finding problem. This algorithm does not handle corner-cases where $c_{py}c_{po} = 0$, but these can be dealt with on case-by-case basis as needed. From Algorithm 1, we see that there are two potential ways for there to be multiple equilibria: either for a given infection pressure which solves Eq. (21) there are multiple intersection points with the best-response set, or there are multiple solutions to Eq. (21). From the proof of Theorem 3, we know there is at least one solution to Eq. (19) for every solution to Eq. (21).

Let us consider the first possibility that there might be multiple intersection points. If $\widetilde{\lambda} > 0$ is a solution to Eq. (21), the set of aggregate exposure rates that can generate said infection pressure $\widetilde{\lambda}$ is determined by $\psi(\widetilde{\lambda}, \overline{\sigma}_y, \overline{\sigma}_o) = 0$, which describes a hyperbola in $\overline{\sigma}_y$ and $\overline{\sigma}_o$ (see Eq. (40), Appendix A). This hyperbola can never intersect a best-response set more than once if the best-response set has single element. If the best-response set σ^B is not a single element, then from Eq. (10) we know it is one of $\{0\} \times [0,1]$, $\{1\} \times [0,1]$, $[0,1] \times \{0\}$, $[0,1] \times \{1\}$, or $[0,1] \times [0,1]$. In all except the last case, the elementary properties of Cartesian hyperbolas (where the asymptotes parallel the axes) ensure that there is never more than one intersection point. In the last case, where every strategy is a best-response, every strategy yielding a stationary infection pressure satisfying Eq. (21) is a Nash equilibrium. However, this last case can only occur if $\widetilde{\lambda} = 0$ or System (11) is satisfied. In the special case of $\widetilde{\lambda} = 0$, candidate solution strategies are all strategies $\overline{\sigma}$ such that $0 \leq \mathcal{R}(\overline{\sigma}_y, \overline{\sigma}_o) < 1$, with $\mathcal{R}$ given by Eq. (42) (Appendix A). This is a triangular subset of the strategy set $[0,1] \times [0,1]$, which easily allows multiple solutions. In the special case of System (11) being satisfied, the one-dimensional subset of all strategies yielding a stationary infection pressure satisfying Eq. (21) is the set of Nash equilibria. In both cases, the set of equilibria is connected.

The second way multiple equilibria may appear is if there is more than one solution to Eq. (21). In order for there to be multiple solutions, the infection pressure can not be a decreasing function of the aggregated exposure rates $\overline{\sigma}$; there must be a case where reducing exposure increases the infection pressure. Combined with the preceding discussion, we can construct a sufficient condition for there to be a unique Nash equilibrium.

Theorem 4 *Given Hypotheses 1 and 2, if* $\widetilde{\lambda}(\sigma) > 0$ *implies* $\widetilde{\lambda}(\sigma)$ *is strictly increasing in* σ, $c_{py} > 0$, $c_{po} > 0$, *and System* (11) *is not satisfied, then Eq.* (7a) *has a unique Nash equilibrium.*

Proof First, from our conditions, Theorem 3 implies the existence of a Nash equilibrium. Under Hypotheses 1 and 2, Lemma 1 holds. From Lemma 1, $\sigma^B(\lambda)$ is decreasing in λ. If $\widetilde{\lambda}(\sigma)$ is increasing in σ, then $\widetilde{\lambda}(\sigma^B(\lambda))$ is decreasing in λ. This implies that Eq. (21) can have only one solution. Since $c_{py} > 0$ and $c_{po} > 0$, Hypothesis 1's requirement for $\mathcal{R}_0 > 1$ ensures $\lambda(\sigma^B(0)) > 0$. This means the solution of Eq. (21) must be positive. Since System (11) is not satisfied, the best-response sets must always lie on the boundary of the $[0,1] \times [0,1]$ excluding $\{\sigma : \widetilde{\lambda}(\sigma) = 0\}$. Then the strict-monotonicity of $\widetilde{\lambda}(\sigma)$ is sufficient to ensure only a single best-response can match the infection pressure. QED

It is dissatisfying to require infection-pressure monotonicity – this seems like something that can be demonstrated from our model. Perhaps surprisingly, the infection pressure *is not* always monotone. The monotonicity

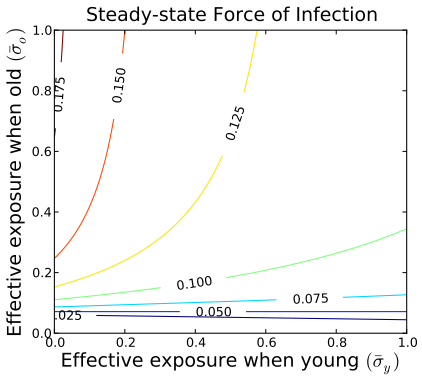

Fig. 2 The infection pressure $\widetilde{\lambda}$, as shown in this contour plot, depends on the components of the aggregate strategy $\overline{\sigma}$ for parameter values given in Eq. (23). The infection pressure is not always monotone increasing in $\overline{\sigma}$. The age-dependent transmission rate interacts with the shortened lifespan, such that the infection pressure is maximized by minimizing the effective exposure of the young.

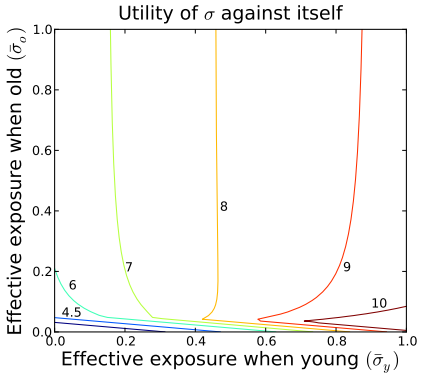

Fig. 3 Contour plots of the utility $\mathcal{U}(\overline{\sigma}, \widetilde{\lambda}(\overline{\sigma}))$ as it depends on the aggregate strategy $\overline{\sigma}$. Corresponding infection pressures are shown in Fig. 2. The utility is maximized when the old age-group invests sufficiently to induce herd-immunity, while the young invest nothing. Parameter values given in Eq. (23).

of the infection pressure is discussed in Appendix A, and a condition for when the infection pressure is increasing is given by Eq. (49). But this condition does not always hold.

For example, if $\beta_y = 0$, increasing juvenile exposure may decrease the infection pressure. To be specific, consider the following parameter set:

$$\begin{aligned} u_y =& u_o = 1,\ c_{py} = 1,\ c_{po} = 1,\ c_{iy} = 1,\ c_{io} = 0.58, \\ r = 1,\ \beta_y =& 0,\ \beta_o = 0.06,\ m_y = 0.005,\ m_o = 0.010,\ \gamma_y = 0.3,\ \gamma_o = 0.3,\ f = 0.1. \end{aligned} \tag{23}$$

In the absence of infection, the system converges to a steady-state where 9% of the population is young and 91% is old. Infection shortens individual lifespans dramatically at both ages. Only the old transmit the disease significantly, though both age groups may be exposed. Infection itself is more costly in the young. The costs of prevention are equal in both groups. This leads to a non-monotone infection pressure as a function of the aggregate exposure rates (Figure 2). The maximum infection pressure occurs when young people have no exposure but old people are completely exposed. Solutions of Eq. (21) are plotted in Figure 4(left) for a range of infection costs to the old. Of particular note, there is an intermediate range of costs including $c_{io} = .58$ where there are three coexisting solutions. This is shown in Figure 4(right).

The 3 solutions of Eq. (21) under Eq. (23) correspond to 3 candidates for game equilibria. Each of these is a Nash equilibrium (see Figure 5), although the middle candidate is only a weak Nash equilibrium. Because prevention is too expensive, old individuals never have personal incentive to invest in prevention, and $\sigma_o^B = 1$ independent of λ. Since only the old transmit infection, the young can not avoid some risk of infection. If all young individuals protect themselves, the infection pressure is maximized, and diverging from the aggregate behavior by allowing larger effective exposure rates increases the individual's risk of infection sufficiently for

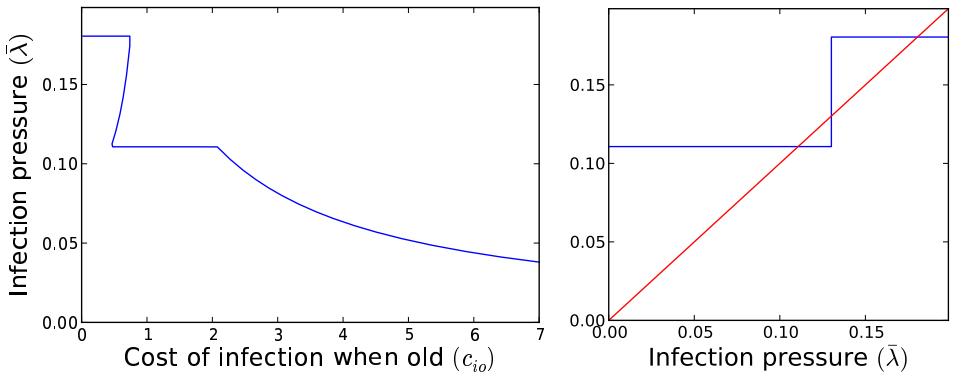

Fig. 4 Here (left), we show a plot of the solutions of Eq. (21) as c_{io} is varied. Except for the narrow region when $c_{io} \in [.46, .61]$, there is a unique solution of Eq. (21) corresponding to a unique Nash equilibrium. (right) An illustrative plot of the inclusion relation given by Eq. (21) when $c_{io} = 0.58$. The three intersection points determine three infection pressures corresponding to Nash equilibria. The three Nash equilibria corresponding to the solutions of Eq. (21) and along with their infection pressures are $(\sigma^*, \bar{\lambda}) \in \{(\langle 1, 1\rangle, 0.110), (\langle 0.47, 1\rangle, 0.13), (\langle 0, 1\rangle, 0.18)\}$

the action to be a net loss. If no young individual protects themselves, than the infection pressure is reduced sufficiently that the expected cost of infection is less than the expected cost of prevention. Thus, there can be two distinct strong Nash equilibria under the specified conditions. There is also a third weak Nash equilibrium lying between these two. Numerical calculations show that the dynamic steady-states of the epidemic process are locally stable for the effective exposure rates of each game equilibrium. The middle equilibrium does not have local invasion potential and can be displaced by either of the other two equilibria (see Figure 5). Each of the corner equilibria can invade near-by strategies, but neither has global invasion potential (see Figure 5). Thus, the game-theory analysis predicts that behaviors corresponding to one of these two corner equilibria could be observed in practice, but provides no insight into which will be selected.

Our analysis of this two-stage social distancing model reveals that the sensitivity of infection pressure to behavioral changes is key in determining the configurations of game equilibria. In practice, the specific nature of changes to infection pressure will depend on the contact patterns. However, we have made use of some rather restrictive hypotheses concerning infection pressure in obtaining our results. Our hypotheses are satisfied if infection pressure is uniform in both age groups, the transmission rate is decreasing with age and disease-mortality is increasing with age, but we know this is not generally true. In particular, many viral infections have higher mortalities in the young than in the old. As such, in order to apply our methods in many real-world situations, it seems that greater model detail, with additional information, will be needed. Toward this end, we will now introduce a model with continuous age-structure.

3 Continuous age structure

We can generalize from the minimal 2-stage scenario to models with continuous sequential demographic structure, while extending Hypotheses 1 and 2 in a natural way. Let the population-scale dynamics are governed by the coupled McKendrick–von Forrester equations. In addition to age-since-birth, we will also track age-since-infection. Under Hypothesis 2, the infection pressure λ is a rank-1 linear function of the age-distribution of infections. For an SI epidemic, then, the dynamic equations may be formulated

$$\frac{\partial S}{\partial t} + \frac{\partial S}{\partial a} = -\mu(a)S - \overline{\sigma}(a)\lambda S, \quad S(a=0,t) = r, \tag{24a}$$

$$\frac{\partial I}{\partial t} + \frac{\partial I}{\partial a} + \frac{\partial I}{\partial z} = -\gamma(a,z)I, \quad I(a,t,z=0) = \overline{\sigma}(a)\lambda S(a,t), \tag{24b}$$

$$\lambda = \int_0^{a_{\max}} \int_0^a \beta(a,z)I(a,t,z)\mathrm{d}z\mathrm{d}a. \tag{24c}$$

where a is the age-since-birth, z is the age-since-infection, $\overline{\sigma}(a)$ is the aggregate effective exposure rate at age a, and $\beta(a,z)$ is the transmission rate as a function of ages. Consistent with Hypothesis 1, we constrain the

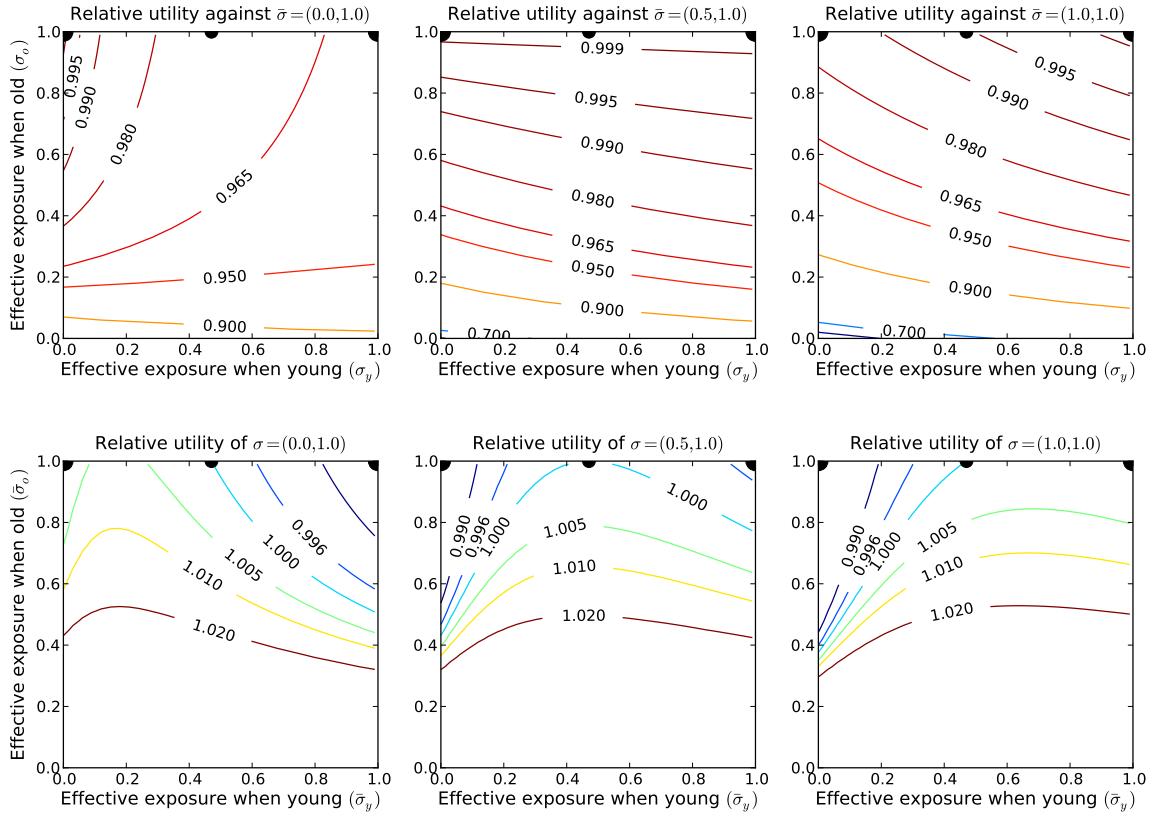

Fig. 5 Contour plots of response utility (top row) and relative invasion potentials (bottom row) of the three candidate equilibria identified in Figure 4(left). The equilibria locations are marked by the black dots. All three are global Nash equilibria because no individual strategy has a relative utility greater than 1 when played against the candidate (top row). The Nash equilibrium $\langle .5, 1\rangle$ is a weak equilibrium, as other strategies have relative utility equal to 1 when played against $\langle .5, 1\rangle$. The other two are strong equilibria. None of the three Nash equilibria has global invasion potential, as $\langle 0, 1\rangle$ can not invade $\langle 1, 1\rangle$, $\langle 1, 1\rangle$ can not invade $\langle 0, 1\rangle$, and $\langle .5, 1\rangle$ can invade neither of the other two. None of these equilibria correspond to the optimal community behavior (see Figure 3), and in fact, $\langle 0, 1\rangle$ **maximizes** the infection pressure. Parameter values given in Eq. (23).

removal rates $\mu(a)$ and $\gamma(a, z)$ such that both are positive and strictly increasing for sufficiently large a, with $\mu(a) \le \gamma(a, 0) \le \gamma(a, z)$ for $z \ge 0$. To avoid complications associated with infinite-horizons, we assume there is a finite age $a_{\max}$ such that $\mu(a \ge a_{\max}) = \infty$. Again, we make the simple assumption that susceptible individuals are born at a constant rate r. This model is one of the generalizations of SIR theory originally suggested by Kermack and McKendrick (1933).

Stationary solutions can be identified by finding infection pressures $\widetilde{\lambda}$ satisfying the equation

$$\widetilde{\lambda} = \widetilde{\lambda} \int_0^{a_{\max}} \int_0^a \beta(a, z)\overline{\sigma}(a - z) r e^{-\int_0^{a-z} \overline{\sigma}(t)\widetilde{\lambda} + \mu(t)\mathrm{d}t} e^{-\int_0^z \gamma(a-z+t,t)\mathrm{d}t} \mathrm{d}z\mathrm{d}a. \tag{25a}$$

and calculating

$$S(a) = r e^{-\int_0^a \overline{\sigma}(t)\widetilde{\lambda} + \mu(t)\mathrm{d}t}, \tag{25b}$$

$$I(a, z) = \overline{\sigma}(a - z)\widetilde{\lambda} S(a - z) e^{-\int_0^z \gamma(a-z+t,t)\mathrm{d}t}. \tag{25c}$$

The disease-free state corresponding to $\widetilde{\lambda} = 0$ is always a solution of Eq. (25a). After defining

$$F(\lambda, \overline{\sigma}) := \int_0^{a_{\max}} \int_0^a \beta(a, z)\overline{\sigma}(a - z) r e^{-\int_0^{a-z} \overline{\sigma}(t)\lambda + \mu(t)\mathrm{d}t} e^{-\int_0^z \gamma(a-z+t,t)\mathrm{d}t} \mathrm{d}z\mathrm{d}a, \tag{26}$$

other stationary solutions can be identified by solving $F(\widetilde{\lambda},\overline{\sigma})=1$. By inspection, we can see that the integrand is non-negative, and also that $F(\lambda,\overline{\sigma})$ is a decreasing function of λ such that $F(\infty,\overline{\sigma})=0$. If $F(0,\overline{\sigma})<1$, then there are no stationary solutions with positive infection pressures, while if $F(0,\overline{\sigma})>1$, then there is a unique stationary solution with a positive infection pressure.

Just as in the two-stage model, there is a system of linear differential equations describing the probability that an individual is susceptible or infected at age a ($P_S(t,a)$ and $P_I(t,a)$ respectively). They are closely related to System (24), and given by

$$\frac{\partial P_S}{\partial t}=-\frac{\partial P_S}{\partial a}-\mu(a)P_S-\sigma(a)\widetilde{\lambda}P_S,\quad P_S(t=t_0,a)=\delta(a), \tag{27}$$

$$\frac{\partial P_I}{\partial t}=-\frac{\partial P_I}{\partial a}-\frac{\partial P_I}{\partial z}-\gamma(a,z)P_I,\quad P_I(t,a,z=0)=\sigma(a)\widetilde{\lambda}P_S(t,a), \tag{28}$$

where t_0 is the date-of-birth, and $\delta(a)$ refers to a Dirac delta-function. The delta-function initial condition means we could simplify this system to an ordinary differential equation along the characteristics. However, it will be convenient for the Lagrangian approach that follows to keep age and time as independent coordinates.

The goal of an individual, then is to find a strategy that will maximize her/his lifetime expected utility, given that each individual is born susceptible. But the individual's strategy must be consistent with the actions of all other players. Formally, this defines a population game where we seek to find equilibrium strategy $\overline{\sigma}(a)$ and stationary infection pressure $\widetilde{\lambda}$ such that

$$\overline{\sigma}=\underset{\sigma}{\operatorname{argmax}}\ \mathcal{U}(\sigma),\quad \text{with} \tag{29a}$$

$$\mathcal{U}(\sigma)=\int_{t_0}^{t_0+a_{\max}}\int_0^{a_{\max}}e^{-ha}\left\{[u_S(a)-(1-\sigma(a))c_p(a)]P_S(t,a)+\int_0^a u_I(a,z)P_I(t,a,z)\mathrm{d}z\right\}\mathrm{d}a\mathrm{d}t, \tag{29b}$$

where $u_I(a,z)$ is the rate of utility gain at age a after having been infected for time $z\le a$ and is a positive function, and where the utility gain for susceptibles $u_S(a)$ is never less than that of an infected individual of the same age ($u_S(a)\ge u_I(a,z)$ for all ages a,z), and $c_p(a)$ is the minimum investment needed to stop personal exposure at age a. We are studying the special-case of a stationary infection pressure, transition rates, and population dynamics, so the utility $\mathcal{U}$ will have the same value for all birth-dates t_0 and without lose of generality, we take $t_0=0$.

In general, our population game need-not have pure-strategy equilibria satisfying (29) (Houston and McNamara, 1999), but we will proceed under the assumption that our particular game does. Since individuals in the game are solving a constrained optimization problem, we can put this in Lagrangian form, and attempt to identify game equilibria by looking for values of $\widetilde{\lambda}$ where Eq. (29) is satisfied. The Lagrangian of our game's constrained optimization is

$$\begin{aligned}\mathscr{L}=&\int_0^\infty\int_0^{a_{\max}}e^{-ht}\left\{[u_S(a)-(1-\sigma(a))c_p(a)]P_S(t,a)+\int_0^a u_I(a,z)P_I(t,a,z)\mathrm{d}z\right\}\mathrm{d}a\mathrm{d}t\\&-\int_0^\infty\int_0^{a_{\max}}V_S(t,a)\left\{\left[\sigma(a)\lambda+\mu(a)\right]P_S(t,a)+\frac{\mathrm{d}P_S}{\mathrm{d}t}+\frac{\mathrm{d}P_S}{\mathrm{d}a}\right\}\mathrm{d}a\mathrm{d}t\\&-\int_0^\infty\int_0^{a_{\max}}\int_0^a V_I(t,a,z)\left[\frac{\mathrm{d}P_I}{\mathrm{d}t}+\frac{\mathrm{d}P_I}{\mathrm{d}a}+\frac{\mathrm{d}P_I}{\mathrm{d}z}+\gamma(a,z)P_I(t,a,z)-\delta(z)\sigma(a)\lambda P_S(t,a)\right]\mathrm{d}z\mathrm{d}a\mathrm{d}t\end{aligned} \tag{30}$$

where $V_S(t,a)$ and $V_I(t,a,z)$ are the adjoint functions. Because of the confluence of age and time, along with the boundary conditions, we find it clearer to work with the Lagrangian rather than the Hamiltonian.

The evolution of the adjoint variables can be specified by setting the functional-derivatives (see Appendix C) of the Lagrangian with respect to the individual's state to zero, as

$$0=\frac{\delta\mathscr{L}}{\delta P_S},\ 0=\frac{\delta\mathscr{L}}{\delta P_I}. \tag{31}$$

This leads to a weak differential-equation form for equations governing the evolution of the adjoint variables,

$$-\frac{\partial V_S}{\partial a} = u_S(a) - [1-\sigma(a)]c_p(a) + \widetilde{\lambda}\sigma(a)V_I(a,0) - \left[h + \widetilde{\lambda}\sigma(a) + \mu(a)\right] V_S(a) \tag{32a}$$

$$-\frac{\partial V_I}{\partial a} - \frac{\partial V_I}{\partial z} = u_I(a,z) - [h+\gamma(a,z)]\, V_I(a,z) \tag{32b}$$

with terminal conditions $V_S(a_{\max}) = V_I(a_{\max}, z) = 0$. The time variable t is redundant with the age a when population dynamics are at steady-state, and has been dropped to simplify our notation.

The integrated form of System (32) can also be derived directly from first-principles, without having to consider the details of the Lagrangian. At a certain age a and a certain age-of-infection z, the value of the infected state

$$V_I(a,z) = \int_0^{a_{\max}-a} e^{-\int_0^w \gamma(a+v,z+v)\mathrm{d}v}\gamma(a+w,z+w)\int_0^w u_I(a+v,z+v)e^{-hv}\mathrm{d}v\mathrm{d}w \tag{33a}$$

$$= \int_0^{a_{\max}-a} e^{-\int_0^w h+\gamma(a+v,z+v)\mathrm{d}v} u_I(a+w,z+w)\mathrm{d}w. \tag{33b}$$

The second form here is obtained by integration-by-parts of the first under the condition that

$$e^{-\int_0^{a_{\max}-a}\gamma(a+v,z+v)\mathrm{d}v} = 0, \tag{34}$$

and can also be obtained from integration of Eq. (32b). The susceptible state then has value

$$V_S(a;\sigma,\widetilde{\lambda}(\overline{\sigma})) = \int_a^{a_{\max}} e^{-\int_a^\alpha \widetilde{\lambda}\sigma(t)+\mu(t)\mathrm{d}t}\left[\widetilde{\lambda}\sigma(\alpha)+\mu(\alpha)\right]\times \left\{e^{-h(\alpha-a)}\left(\frac{\widetilde{\lambda}\sigma(\alpha)V_I(\alpha,0)+\mu(\alpha)0}{\widetilde{\lambda}\sigma(\alpha)+\mu(\alpha)}\right) + \int_a^\alpha [u_S(v)-(1-\sigma(v))c_p(v)]\, e^{-h(v-a)}\mathrm{d}v\right\}\mathrm{d}\alpha \tag{35a}$$

$$= \int_a^{a_{\max}} e^{-\int_a^v h+\widetilde{\lambda}\sigma(t)+\mu(t)\mathrm{d}t}\left[u_S(v)-(1-\sigma(v))c_p(v)+\widetilde{\lambda}\sigma(v)V_I(v,0)\right]\mathrm{d}v \tag{35b}$$

where the second form is again obtained by integration-by-parts from the first, and is the solution to Eq. (32a).

The value of the susceptible state depends on the stationary infection pressure $\widetilde{\lambda}$ as well as the individual's behavior, as described by $\sigma(a)$.

The utility $\mathcal{U} = V_S(a=0;\sigma,\lambda(\overline{\sigma}))$. As usual, the utility defines a game $\mathcal{U}(\sigma,\overline{\sigma})$ since the best strategy depends on the infection pressure, which in turn depends on the common behavior $\overline{\sigma}$. The best response correspondence $\sigma^B(a)$ that maximizes the value of being susceptible at a given age is determined by the switching conditions

$$\sigma^B(a;\widetilde{\lambda}) = H\left(c_p(a) + [V_I(a,0) - V_S(a;\sigma^B,\widetilde{\lambda})]\widetilde{\lambda}\right). \tag{36}$$

This is derived from maximizing the rate of increase of Eq. (32a) over possible values of $\sigma(a)$ for each a. The value of $\sigma^B(a)$ depends only on other components of the best response, but only those choices made at older ages, $\sigma^B(\hat{a} > a)$, needed to evaluate Eq. (35).

From the best responses, we obtain the equilibrium condition

$$\sigma^* \in \sigma^B(\widetilde{\lambda}(\sigma^*)). \tag{37}$$

We would like to extend our results from the two-stage case to this more general setting.

Lemma 2 *If $V_I(a,0) < \inf_\lambda V_S(a;\sigma^B,\lambda)$, then $\sigma^B(a;\widetilde{\lambda})$ is an decreasing function of $\widetilde{\lambda}$.*

This is easily proven by inspection of Eq. (36). This naturally leads to speculation concerning the generalization of Theorem 4.

The Monotone Infection Pressure Conjecture *If $V_I(a,0) < \inf_\lambda V_S(a;\sigma^B,\lambda)$ for all a, $\widetilde{\lambda}(\sigma)$ is increasing in σ, and $\mathcal{U}$ is not too flat, then there is a unique Nash equilibrium.*

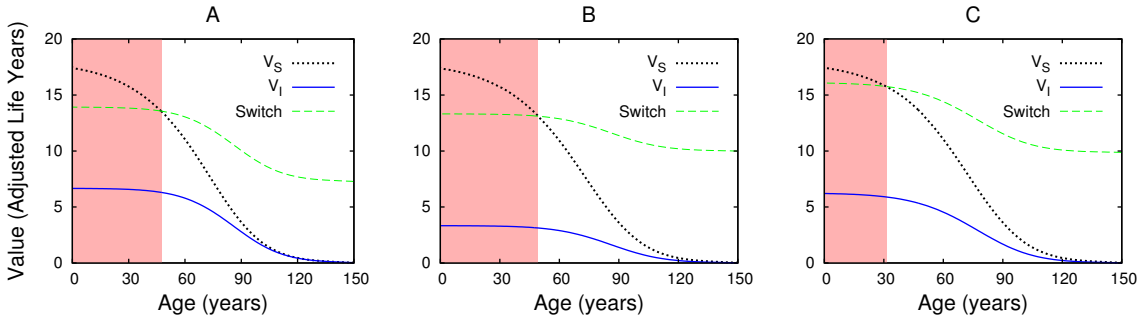

Fig. 6 Regions of game equilibrium social distancing and the associated values of the susceptible and infected states when the conditional life-expectancy under infection is $u_I = 1$, $c_p = 0.1$, $\zeta = 0.1$ (A), $u_I = 0.5$, $c_p = 0.1$, $\zeta = 0.1$ (B), and $u_I = 0.5$, $c_p = 0.1$, $\zeta = 0.03$ (C). The red regions represent the ages during which social-distancing is optimal, while the intersections of the black and green curves identify the boundaries of the ages of social distancing. Comparing plots (A) and (B), we see that disability-costs associated with infection have little effect on the equilibrium behavior, despite significant reducing the well-being of infected individuals. Comparing plots (B) and (C), we see that a 3-fold reduction in the disease mortality rate (while β is reduced 3-fold to keep $R_0 = 5$) reduces the duration of social-distancing from 50 years to 30 years. Thus death seems to be having a greater impact on equilibrium behavior than disability.

An argument would go along the same lines as Theorem 4, and follows from Lemma 2. However, in the continuum model, more care is needed in handling the potential for singular solutions, where $\mathcal{U}$ might become degenerate.

A comprehensive analytic treatment of this model would be a substantial undertaking. Instead, let us close with a numerical exploration of one reasonable case similar to HIV in a human population. To parameterize our model, we need to specify the details of demography, transmission, removal, and costs. Based on CDC's mortality schedule for the US in 2003 (Arias, 2006), the mortality rate for generic individuals in the US is approximated by the singularized Gompertz model

$$\mu(a) = \exp(k_0 + k_1 a)\left(1 + \frac{\epsilon}{\sqrt{a_{\max} - a}}\right) \tag{38}$$

where $k_0 \approx -9.46$, $k_1 \approx 0.085$, $\epsilon = 0.01$, and $a_{\max} = 150$. We normalize our population structure by taking the birth rate $r = 1$. Under these hypotheses, the total population size in the absence of infection is given by

$$N \approx r\mathrm{Ei}_1\left(\frac{e^{k_0}}{k_1}\right)\frac{e^{e^{k_0}/k_1}}{k_1} \approx 75.5 \tag{39}$$

where $\mathrm{Ei}_1(x)$ is the exponential integral (Abramowitz and Stegun, 1972).

For disease transmission, we make the simplest mathematical hypotheses. We assume the transmission rate is a constant, independent of age or age-of-infection $\beta(a, z) := \beta$. We assume that the removal rate is the same as natural mortality except for the addition of a constant, so $\gamma(a, z) := \mu(a) + \zeta$. For untreated HIV, $1/\zeta \approx 10$ years. This duration would be much larger under highly-active anti retroviral therapy. The transmission rate is calibrated in all our simulations so that the basic reproduction number $\mathcal{R}_0 \approx 5$. For accounting, we take the direct value of a year of life as susceptible $u_S = 1$, and adopt a background annual discount-rate of about 5 percent, so $h = 0.05$.

Under these assumptions, best-responses to specific epidemiological scenarios can be calculated. The Nash equilibrium condition (37) can be solved by iteration or (for this special case) root-finding. Examples are shown in Figure 6. Under the proposed assumptions, the calculation is particularly simple because there is a single switching event that is needed to represent the best-response functions. In general, the switching structure may be quite complicated, making Eq. (37) quite difficult to solve.

4 Discussion

This concludes our initial explorations of epidemiological games in which individual strategies are age-structured, thereby extending the work of Reluga et al. (2007). As expected, the analysis of this game with vector strategies is more difficult than the analysis of games with scalar strategies, even for the simplest SI epidemic theory. However, our scenario is tractable, and we are able to obtain reasonably complete numerical results

despite a currently-incomplete theoretical analysis. In both games of two-stage age structure and continuous age structure, a utility function of individual strategy choice for an individual initially susceptible is defined when the transmission-dynamics are near steady-state. The existence of Nash equilibria has been discussed in a few special cases for both the two-age class and the continuous-age class models. The determination of Nash equilibria for the two-stage case is complemented by a numerical algorithm. Regarding the uniqueness of Nash equilibrium, our primary result is that relationships between behavior change and infection pressure have key impacts on the equilibria-structure of the game. If the infection pressure decreases uniformly with social distancing, then there is a unique equilibrium. But infection pressure is not necessarily decreased by social distancing, even in the simplest scenarios. We provide one such example, and document how the counter-intuitive aspects of social distancing can result in the coexistence of multiple Nash equilibria.

Non-uniqueness of Nash equilibria has also been previously observed in Reluga et al. (2007) for the SIR model where virulence is age-dependent but behaviors are not age-dependent. Here, we study age-dependent behaviors which can be influenced by all other factors including the transmission rates, the virulence, the cost of infections, the cost of investment, and the infection pressure when one individual makes behavioral choices to maximize his/her utility. Therefore, unlike Reluga et al. (2007) in which infected individuals can recover and become immune for the rest of their lives, infected individuals must bear the burden of infection for their entire lives. This would seem to remove the benefits of early infection, but the analysis presented here reveals that feedbacks between social distancing and the force of infection themselves can be sufficient to preclude any equilibrium strategy from having global invasion potential. To better understand of the relationships between infection pressure and social distancing behavior, we need to understand complications arising from disease-specific features including transmission, virulence, and the impact of social distancing on disease dynamics. In applications, we may be able to make significant progress using numerical approaches, but should be aware that strong asymmetries in mixing and transmission may complicate the identification of equilibria.

While we have a strong hold on the problem of numerical calculation of Nash equilibria for (7a), the analytical characterization of these equilibria is not yet complete. We have exact solutions in the extreme cases of free social distancing and expensive social distancing, but for intermediate cases we only show that these exists at least one Nash equilibrium. Analytically, we do not have exact expressions for these Nash equilibria. Nor do we establish that there are at most three equilibria. We would also like to characterize equilibria without the restrictions of Hypothesis 2, and to provide a condition for an evolutionary stable strategy. In many models, the mixing patterns among age groups lead to more complex formulations for age-specific infection pressures. The game theoretic analysis of such models may proceed similar to that presented here. However, general results regarding the determination of Nash equilibria are harder to obtain because the corresponding fixed-point equations can not be reduced to one-dimension, where particularly powerful mathematical methods are available.

Our analysis hopefully provides useful guidance to researchers investigating epidemiological games in specific practical scenarios with different infectious disease dynamics and reasonably well-characterized parameters. While it may be hard to obtain symbolic characterizations of the equilibria, numerical procedures should provide useful results. When constructing steady-states, it is important to remember to assess the dynamic stability of the steady states at least numerically. If there are steady-states of interest that are not stable, then the style of analysis used here is inadequate, and more general methods such as differential game theory (Reluga, 2010) or mixed-strategy equilibria may provide better solutions. Issues of mixed-strategy usage, heterogeneous populations, and error-prone decision making may be important for these models, given the absence of a unique game equilibria under some parameter values. The linear dependence of the reduction in exposure risk on the individual investment cost is one of the simplified considerations here. A more general case where nonlinear dependence is allowed, as can be expected in practice, would possibly also complicate the Nash equilibrium structures. The differences in relative utility shown in Figure 5 are relatively small between equilibria, and consideration of trembling-hand effects where players make random errors may make non-uniqueness results moot. We will try to explore these issues further in the future.

Acknowledgements

This research was funded in part by National Science Foundation Grant DMS-0920822 (TCR), the Bill and Melinda Gates Foundation Grant Number 49276 (TCR) and National Institutes of Health grant PAR-08-224 (TCR,JL). Portions of this work were first presented at the 2008 Society for Mathematical Biology annual meeting. We would like to thank an anonymous reviewer for useful suggestions, including the simplification of Equations 33 and 35.

References

Abramowitz, M., Stegun, I.A. (eds.): Handbook of Mathematical Functions with Formulas, Graphs, and Mathematical Tables. 10th edn. National Bureau of Standards, Washington, D.C. (1972)

Arias, E.: United states life tables, 2003. National Vital Statistics Reports **54**(14) (2006)

Aubin, J.P.: Mathematical Methods of Game and Economic Theory. Dover (1979)

Brito, D.L., Sheshinski, E., Intriligator, M.D.: Externalities and compulsory vaccinations. Journal of Public Economics **45**, 69–90 (1991)

Bunimovich-Mendrazitsky, S., Stone, L.: Modeling polio as a disease of development. Journal of theoretical biology **237**(3), 302–315 (2005)

Charlesworth, B.: Evolution in Age-structured Populations. Cambridge University Press, New York, NY (1994)

Clark, C.W., Mangel, M.: Dynamics State Variable Models in Ecology: Methods and Applications. Oxford University Press, New York, NY (2000)

Chen, F.H.: Rational behavioral response and the transmission of stds. Theoretical Population Biology **66**(1), 307–316 (2004)

Chen, F.H.: A susceptible-infected epidemic model with voluntary vaccinations. Journal of Mathematical Biology **53**(1), 253–272 (2006)

Cornforth, D.M., Reluga, T.C., Shim, E., Bauch, C.T., Galvani, A.P., Meyers, L.A.: Erratic flu vaccination emerges from short-sighted behavior in contact networks. PLOS Computational Biology (2011)

Diekmann, O., Heesterbeek, J.A.P., Metz, J.A.J.: On the definition and the computation of the basic reproduction ratio R_0 in models for infectious diseases in heterogeneous populations. Journal of Mathematical Biology **28**(4), 365–382 (1990)

Donoghue, J. F., Golowich, E., and Holstein, B. R. *Dyamics of the Standard Model.* Cambridge University Press, Cambridge, UK, 1996.

Houston, A., McNamara, J.: Models of Adaptive Behaviour. Cambridge University Press, Cambridge, UK (1999)

Kermack, W.O., McKendrick, A.G.: Contributions to the mathematical-theory of epidemics. III. further studies of the problem of endemicity. Proceedings of the Royal Society of London **141**(843), 94–122 (1933)

McNamara, J.M., Houston, A.I., Collins, E.J.: Optimality Models in Behavioral Biology. SIAM Review **43**(3), 413–466 (2001)

Reluga, T.: Game theory of social distancing in response to an epidemic. PLOS Computational Biology **6**(5), e1000793 (2010). DOI 10.1371/journal.pcbi.1000793

Reluga, T.C.: An SIS game with two subpopulations. Journal of Biological Dynamics **3**(5), 515–531 (2009)

Reluga, T.C., Galvani, A.P.: A general approach for population games with application to vaccination. Mathematical Biosciences **230**(2), 67–78 (2011)

Reluga, T.C., Medlock, J., Poolman, E., Galvani, A.P.: Optimal timing of disease transmission in an age-structured population. Bulletin of Mathematical Biology **69**(8), 2711–2722 (2007)

Rzewuski, J.: Field Theory. Hafner Publishing Company, New York, USA (1969)

Schenzle, D.: An age-structured model of pre-and post-vaccination measles transmission. Mathematical Medicine and Biology **1**(2), 169–191 (1984)

van den Driessche, P., Watmough, J.: A simple SIS epidemic model with a backward bifurcation. Journal of Mathematical Biology **40**(1), 525–540 (2000)

A Steady-state analysis

We only address the steady-state analysis under Hypothesis 2. This simplifies the problem by making it easy to reduce the stationary solution analysis to a scalar root-finding problem.

At a stationary solution, the infection pressure $\widetilde{\lambda}$ solves the cubic steady-state equation $\widetilde{\lambda}\psi(\widetilde{\lambda};\overline{\sigma}_y,\overline{\sigma}_o)=0$, where

$$\psi(\lambda;\overline{\sigma}_y,\overline{\sigma}_o) := \left(\lambda+\frac{m_o}{\overline{\sigma}_o}\right)\left[\gamma_o\left(\lambda\,\overline{\sigma}_y+m_y+f\right)\left(\gamma_y+f\right)-r\overline{\sigma}_y\left(f\beta_o+\gamma_o\beta_y\right)\right]-f\beta_o r\left(\gamma_y+f\right). \tag{40}$$

The disease-free stationary solution (DFSS) is

$$(S_y,I_y,S_o,I_o)=\left(\frac{r}{m_y+f},0,\frac{rf}{(m_y+f)m_o},0\right). \tag{41}$$

Linearizing around the DFSS, the reproduction ratio $\mathcal{R}$ is the largest eigenvalue of next generation matrix (van den Driessche and Watmough, 2000; Diekmann et al., 1990), or

$$\mathcal{R} = \frac{\overline{\sigma}_y \beta_y r}{(\gamma_y + f)(f + m_y)} + \frac{\overline{\sigma}_y \beta_o r f}{(\gamma_y + f)(f + m_y)\gamma_o} + \frac{\overline{\sigma}_o \beta_o r f}{\gamma_o m_o (f + m_y)}. \tag{42}$$

In the absence of reductions in exposure, the basic reproduction ratio

$$\mathcal{R}_0 = \frac{\beta_y r}{(\gamma_y + f)(f + m_y)} + \frac{\beta_o r f}{(\gamma_y + f)(f + m_y)\gamma_o} + \frac{\beta_o r f}{\gamma_o m_o (f + m_y)} \tag{43}$$

The disease-free stationary solution is locally asymptotically stable when $\mathcal{R} \leq 1$.

When $\overline{\sigma}_y \overline{\sigma}_o > 0$ and $\mathcal{R} > 1$, there is one positive root and one negative root to $\psi(\lambda) = 0$ because $\psi''(\lambda) > 0$ and $\psi(0) < 0$. Thus, we can define the stationary infection pressure as

$$\widetilde{\lambda}(\overline{\sigma}_y, \overline{\sigma}_o) = \begin{cases} 0 & \text{if } \mathcal{R}(\overline{\sigma}_y, \overline{\sigma}_o) \leq 1, \\ \text{the unique positive solution of } \psi(\lambda; \overline{\sigma}_y, \overline{\sigma}_o) = 0 & \text{if } \mathcal{R}(\overline{\sigma}_y, \overline{\sigma}_o) > 1. \end{cases} \tag{44}$$

A little bit more analysis shows that $\widetilde{\lambda}$ is bounded above; as long as $\gamma_y > m_y$ and $\gamma_o > m_o$, the stationary infection pressure

$$\widetilde{\lambda} < \beta_y \frac{r}{m_y + f} + \beta_o \frac{r}{m_y + f} \frac{f}{m_o}. \tag{45}$$

If $\widetilde{\lambda} > 0$, the corresponding endemic stationary solution

$$S_y = \frac{r}{\widetilde{\lambda}\,\overline{\sigma}_y + m_y + f}, \tag{46a}$$

$$I_y = \frac{r\widetilde{\lambda}\,\overline{\sigma}_y}{\left(\widetilde{\lambda}\,\overline{\sigma}_y + m_y + f\right)(\gamma_y + f)} \tag{46b}$$

$$S_o = \frac{rf}{\left(\widetilde{\lambda}\overline{\sigma}_y + m_y + f\right)\left(\widetilde{\lambda}\overline{\sigma}_o + m_o\right)} \tag{46c}$$

$$I_o = \frac{rf\lambda\overline{\sigma}_y}{\gamma_o(\lambda\overline{\sigma}_y + m_y + f)(\gamma_y + f)} + \frac{rf\lambda\overline{\sigma}_o}{\gamma_o(\lambda\overline{\sigma}_o + m_o)(\lambda\overline{\sigma}_y + m_y + f)} \tag{46d}$$

Local stability can be assessed numerically for specific parameter values. Bunimovich-Mendrazitsky and Stone (2005) present partial stability results of a related model.

To finish this subsection, we will show that the assumption used in Theorem 4 that $\widetilde{\lambda}(\sigma)$ is strictly increasing in σ is possible, but not universal. Implicit differentiation shows that $\partial\widetilde{\lambda}/\partial\overline{\sigma}_o \geq 0$. On the other hand, $\partial\widetilde{\lambda}/\partial\overline{\sigma}_y$ changes sign depending on $\overline{\sigma}_o$ if

$$\frac{(m_y + f)(\gamma_y + f)\gamma_o m_o}{r\beta_o f(\gamma_y - m_y) - r\beta_y(m_y + f)\gamma_o} \in (0, 1), \tag{47}$$

i.e.,

$$\left(\frac{\gamma_y - m_y}{\gamma_o}\right)\left(\frac{f}{m_y + f}\right) > \frac{\beta_y}{\beta_o} + \frac{m_o(\gamma_y + f)}{r\beta_o} > \frac{\beta_y}{\beta_o}. \tag{48}$$

The right-hand inequality is always satisfied, so we really need only consider the left-hand inequality. If

$$\left(\frac{\gamma_y - m_y}{\gamma_o}\right)\left(\frac{f}{m_y + f}\right) < \frac{\beta_y}{\beta_o}, \tag{49}$$

then the infection pressure $\widetilde{\lambda}$ is monotonically increasing in both $\overline{\sigma}_y$ and $\overline{\sigma}_o$. The condition says (in a sense) that the increases in transmission due to a longer lifespan do not outweight reductions in transmission while young. However, the condition requires 6 free parameters, and does not yet have a clear interpretation in biology terms. We do see, though that $\beta_y > \beta_o$ and $\gamma_y < \gamma_o$ is a sufficient conditions for monotonicity.

B Properties of Correspondences

This appendix provides a brief summary of some properties of correspondence relations used in this paper.

A correspondence $f(x) : A \to B$ maps each element of A to a subset of B. Functions are special cases of correspondences. Correspondences can themselves be treated as functions themselves with the power-set of B, $\mathcal{P}(B)$, as their target, but the former definition is often more convenient. Correspondences are a convenient way of describing problems where there may not exist a solution or there may exist multiple solutions, depending on the input arguments. However, because correspondences are multivalued, standard tools such as calculus are not as powerful as they are for single-valued functions.

It is often useful to consider the composition of correspondences. If f is defined as above and $g(x) : B \to C$ is another correspondence, then $g(f(x)) = \{z \in C : \exists y \in f(x) \text{where} z \in g(y)\}$. Correspondence composition respects subset relations, in the sense that if $f(x) \subseteq f(y)$, then $g(f(x)) \subseteq g(f(y))$.

Concepts of continuity must be generalized to deal with correspondences (Aubin, 1979). A correspondence is upper semi-continuous if for any Neighborhood($f(x)$) there exists Neighborhood(x) such that $f(\text{Neighborhood}(x)) \subset \text{Neighborhood}(f(x))$. Upper semi-continuity is preserved under correspondence composition. A correspondences is lower semi-continuous if for any $y \in f(x_0)$ and every Neighborhood(y), there exists Neighborhood(x_0) such that for every $x \in \text{Neighborhood}(x_0)$, $f(x) \cap \text{Neighborhood}(y) \neq \emptyset$. Better mnemonics might be inner=upper and outer=lower semi-continuity, as the first insures the local values describe the values of all arguments in the local neighborhood, and the second insures all neighboring arguments can describe the local values.

Using upper semi-continuity, we can say something useful about the monotonicity of a correspondence. We say that the correspondence f is monotone decreasing if for any $x_a < x_b$, and for all $a \in f(x_a), b \in f(x_b)$, then $a \geq b$. This is a very strong monotonicity condition, as it never allows overlaps other than at the maximum and minimum values of the correspondence, but is useful in our analysis.

C Functional Calculus Methods

When determining our optimality conditions from our Lagrangian, we can make use of a basic understanding of the operations of functional calculus. Functional calculus is an extension of the ideas of multivariable calculus to problems in the framework of calculus of variations, and is a powerful tool of modern physics (Donoghue et al., 1996). The classic examples of it's application are the brachistochrome, isoperimetric problems, and the principle of least action in physics. A rigorous theory of functional calculus is a challenging topic, we'll keep this discussion restricted to the few practical principles we'll use here (for a more detailed discussion of this topic, please refer to (Rzewuski, 1969)).

The basic idea is to extend the concept of a gradient from vectors indexed over a finite set to functions indexed over a continuum using Dirac delta-functions and their derivatives. Let $\theta(x)$ be a function on a space having a finite number of dimensions, with x denoting Cartesian coordinates of a point in this space. The functional derivative of $\theta(x)$ is

$$\frac{\delta\theta(x)}{\delta\theta(y)} = \delta(x-y). \tag{50}$$

We have replaced the standard Leibniz notation of d with δ to emphasis the difference between classical and functional derivatives. The dummy index y represents the component of θ we are differentiating with respect to. The operator on the right hand side of (50) is the functional calculus equivalent of a Jacobian. In this case, it is a delta function peaked when x coincides with y but zero otherwise. In many cases, differentiation will be applied to an integral. For instance,

$$\frac{\delta}{\delta\theta(y)}\int_0^1 \theta(x)dx = \int_0^1 \delta(x-y)dx = \begin{cases} 1 & \text{if } y \in (0,1), \\ \text{undefined} & \text{if } y \in \{0,1\}, \\ 0 & \text{otherwise.} \end{cases} \tag{51}$$

Most of the standard rules of calculus hold for functional differentiation. The derivative of function independent of θ,

$$\frac{\delta f(x)}{\delta\theta(y)} = 0. \tag{52}$$

The product rule holds so

$$\frac{\delta\left[\theta(x_1)\theta(x_2)\right]}{\delta\theta(y)} = \delta(x_1-y)\theta(x_2) + \theta(x_1)\delta(x_2-y), \tag{53}$$

where x_1 are x_2 are two points of the space, and

$$\frac{\delta\theta^n(x)}{\delta\theta(y)} = n\theta^{n-1}(x)\delta(x-y). \tag{54}$$

The chain rule implies

$$\frac{\delta\left[f(\theta(x),x)\right]}{\delta\theta(y)} = \frac{\partial f(\theta(x),x)}{\partial\theta}\,\delta(x-y). \tag{55}$$

In addition to the standard rules of differentiation, the continuity of the index x introduces some properties that are particular to functional calculus. For instance, using integration-by-parts, we can show that

$$\frac{\delta}{\delta\theta(y)}\int f(\theta'(x))dx = \int \frac{\partial f}{\partial\theta'}\frac{\delta\theta'(x)}{\delta\theta}dx = \int \frac{\partial f}{\partial\theta'}\delta'(x-y)dx = -\frac{d}{dx}\left[\frac{\partial f}{\partial\theta'}\right]\Bigg|_{x=y}. \tag{56}$$

We derive rules for functions of higher order derivatives using similar methods.

The rules of functional differentiation are applied to determine critical points of functionals. Given a functional

$$\mathscr{L}[\theta] = \int f(\theta(x),\theta'(x),x)dx, \tag{57}$$

the critical points satisfy

$$\frac{\delta \mathscr{L}[\theta]}{\delta \theta(y)} = 0 \tag{58}$$

for all y. Evaluating the functional derivative,

$$\frac{\delta}{\delta \theta(y)} \int f(\theta(x), \theta'(x), x) dx = \int \frac{\partial f}{\partial \theta} \frac{\delta \theta(x)}{\delta \theta(y)} + \frac{\partial f}{\partial \theta'} \frac{\delta \theta'(x)}{\delta \theta(y)} dx = \left. \frac{\partial f}{\partial \theta} \right|_{x=y} - \frac{d}{dx} \left[\frac{\partial f}{\partial \theta'} \right] \Bigg|_{x=y}, \tag{59}$$

which is just the Euler–Lagrange equation from calculus of variations. Generalizations from a single coordinate x to multiple coordinates can be handled similarly.